SURGERY JOURNAL

SINCE 2000
MEDWELL PUBLICATIONS

CAD SPECT/CT in Managing Liver Tumours and Other Related Abnormalities

[1]F. Usman, [2]R. Zainon, [3]H. Mohammed, [4]K.J. Nizam and [5]B.W. Gbolahan
[1]School of Physics, University Sains Malaysia, Pulau Penang, Penang 11800, Malaysia
[2]Oncological and Radiological Sciences Cluster, Advanced Medical and Dental Institute (AMDI), Universiti Sains Malaysia, 13200 Kepala Batas, Pulau Pinang
[3]Department of Radiology, University of Maiduguri Teaching Hospital, Maiduguri, Nigeria
[4]Nuclear Medicine Unit, AMDI, Universiti Sains Malaysia, Bertam, 13200 Kepala Batas, Pulau Pinang, Malaysia
[5]Integrative Medicine Cluster, AMDI, University Sains Malaysia, Bertam, 13200 Kepala Batas, Pulau Pinang, Malaysia

Key words: Anthropomorphic torso phantom, ^{99m}Tc, SPECT/CT, iterative reconstruction (OSEM), Filtered Back Projection (FBP), CNR, p-value, CAD

Corresponding Author:
Fahad Usman
School of Physics, Universiti Sains Malaysia, Pulau Penang, Penang, 11800, Malaysia

Page No.: 1-9
Volume: 15, Issue 1, 2020
ISSN: 1816-3211
Surgery Journal

Abstract: This research is aimed at evaluating the effect of incorporating OSEM and FBP reconstructed liver SPECT/CT with a modeled CAD system in the management of liver tumors and other radiation induced liver diseases. An Anthropomorphic torso phantom with lung and liver inserts was injected with ^{99m}Tc. The liver and the background were given 0.2 and 0.07 Mbq mL^{-1}, respectively. The lungs inserts were filled with polystyrene beads for humanisation. A mimicked 30 mL tumour (27 mm) in the liver insert was given 2 Mbq mL^{-1}. Sequential SPECT (step and shot, 10 min over 1800 per head) and CT (120 kVp, 80 mAs) projections were acquired using dual head SPECT/16 slice CT system. The projections were reconstructed using OSEM (10 subsets for 2-10 numbers of iterations, Butterworth post filtering, 10 orders and 0.48 frequencies) and FBP (using Butterworth post filtering at 10 order and cut-off frequencies of 0.38-0.58, 0.05 gaps). Segmented and non-segmented SPECT/CT data were obtained. The image j Software made the analysis. Statistical t-test tested the mean grey values of the tumour and its background. The OSEM and FBP reconstructed images were evaluated from their Contrast to Noise Ratio (CNR). The detection ability was evaluated based on 3-5 CNR detection range set by the rose criterion. The t-test showed the background and the tumour's mean values to be statistically significant (p[<]0.05). The CNR values for both modeled and non-modeled CAD FBP images were all under the detection range. Nevertheless, the maximum CNR value was noted at the cutoff frequency 0.48 (1.69).

In OSEM reconstructed images, the peak was observed at around 3-4 numbers of iterations. In accession, its modeled CAD based evaluation gave CNR values within the detection range from 2-8 numbers of iteration with maximum value (4.89) at 4 numbers of iteration. While the detection range was unattainable for the non-modeled CAD OSEM reconstructed liver SPECT/CT. CAD improves liver tumour detection in SPECT/CT imaging. OSEM is the best for tumour detection. In addition, administered activity can be brought down at 4 OSEM's of iterations (40 MLEM iterations) for patient safety. Ultimately, well developed CAD systems are recommended for proper management of liver and its other related abnormalities.

INTRODUCTION

Primary Liver cancers, including both the Hepatocellular Carcinoma (HCC) and the Bile duct cancer (cholangio carcinoma) has been rated among the top cancer types affecting African and Asian regions[1-3]. Furthermore, the mortality rate resulting from its incidence generally increases. Consequently, the need for a reliable means of detecting the cancers is needed in order to improve the survival rate. Nevertheless, early detection of the cancer is problematic because signs and symptoms of liver cancer tend not to be felt or noticed until the cancer is well advanced[4-6]. In gain, proper and accurate sensing of other liver abnormalities assists in the prevention of radiation induced liver disease. This hinders achieving a reasonable survival rate[7, 8].

Many studies have shown the impact of Computed Tomography (CT) and Magnetic Resonance Imaging (MRI) in detecting the incidence and the extent of the cancer as well as other abnormalities. The studies were extended to the incorporation of Computer Aided Detection (CAD) with the imaging modalities[9-11]. Yet, despite all the promising impact of the imaging modalities and CAD systems, a big problem is proper and reliable sensing of the cancers at its early stage[7, 8, 12]. This trouble is less solved by CT and MRI. This is resulted from their capability of reading just the anatomical information of the cancer which its manifestation delays. Single Photon Emission Computed Tomography (SPECT) detects cancers based on the functional and metabolic processes[13, 14]. Thus, it allows the detection of liver cancer and other related abnormalities at their early stage before any anatomical change. Nonetheless, SPECT suffers an inherent low count leading to its poor resolution[14]. Furthermore, it suffers from attenuation, scattering and collimator response effects. Incorporation of SPECT with CT in one outdoor stage has shown and suggested to increase accuracy in the detection of lesions and abnormalities in the liver[15-17]. The CT components play a role of providing both anatomical information as well as an attenuation correction[18-22]. Consequently, an optimal image is obtained. This prevents and manages the occurrence of diseases like Radio Embolisation Induced Liver Disease (REILD) by depicting the exact extent of the tumour to receive the catheter treatment [23-26]. Despite the improvements with SPECT/CT in detecting the lesion, its accurate delineation is unachievable in some cases. The problem is more intense among less experience nuclear medicine physicians and technologists.

This research is aimed at modeling the incorporation of CAD system with the Ordered Subset Expectation Maximization (OSEM) and Filtered Back Projection (FBP) reconstructed SPECT/CT image for the evaluation of the management radioembolisation induced liver disease as well as other liver abnormalities. In addition, quantitative evaluation using Contrast to Noise Ratio (CNR)[27, 28] will be utilised. This is to reduce the difficulties in the medical imaging interpretations among the physicians, especially the less experience ones.

MATERIALS AND METHODS

Subject and data acquisition area: The data acquisition was held at the Nuclear Medicine unit, Clinical trial centre, Advanced Medical and Dental Institute, Universiti Sains Malaysia. The unit is installed with dual camera 16 slice Hybrid SPECT/CT system which was utilised for the image acquisition. The Anthropomorphic Torso phantom with background volume of 10.3 L contains a liver insert (volume 1.2 L), lungs insert (0.9 and 1.1 L for left and right, respectively) and optional cardiac insert. The acquisition of the SPECT/CT Image was conducted with the cardiac insert not in place. The study concentrated on the Liver insert of the phantom. In the liver insert, a tumour was mimicked using a syringe sphere of about 27 mm diameter, volume of about 30 mL. The diameter of such magnitude was taken, so as to prevent the partial volume effect by leaving it to go past the system's spatial resolution which is almost 13 mm FWHM.

SPECT/CT acquisition and its parameters: The SPECT/CT acquisition was performed for 12 min. The step and shoot acquisition mode was used following the injecting the phantom with ^{99m}Tc. The radioactivity concentrations injected were 0.07, 0.2 and 2 Mbq mL^{-1} for the background, liver insert of the phantom and the sphere respectively. Data were acquired using the dual-detector (adjustable) multi-slice (16 slice) CT Scanner (General Electric) equipped with low-energy high-resolution parallel-hole collimators (LEHR). Furthermore, the data were also acquired as 128×128 matrices for 120 projections (60 per gamma

camera head) at 10 seconds/projection using the 'step and shoot mode'. The tomographic projection views were acquired over an arc of 360°. Energy discrimination was accomplished with a 20% energy window centred on 140 keV. The CT component of the examination was acquired immediately after the SPECT component, without changing the phantom arrangement position. The CT was acquired using a diagnostic setting of 120 kVp at 80 mA and 0.8 s. In addition, the unit was set to acquire 3.75 mm thick slices in spiral acquisition mode. This made the data obtained from the CT acquisition perfect for 3D imaging (because of the lack of motion mis-registration) and the increased out of plane resolution (due fastest nature associated with it relative to the conventional method of acquisition). The CT data were acquired into 256×256 matrices. The CT scan was conducted in 2 min this made the total acquisition time for the SPECT/CT, 12 min as mentioned.

SPECT/CT Image reconstruction techniques: The SPECT projections data acquired from the 'step and shoot' acquisition mode were sent to the processing unit of the department. Image processing Personal Computers (PCs) were situated in the unit. The processing PCs were installed with xyleris software containing FBP and OSEM reconstruction capabilities. The data were reconstructed by both the FBP and OSEM reconstruction algorithms, using different parameter selection. For OSEM reconstruction algorithm, the projection data were reconstructed using 10 numbers of subsets with 2-10 numbers of iterations. The post filtration was made using a Butterworth filter, cut-off frequency 0.48 and order 10 for all the OSEM reconstructed images. Also for the FBP reconstruction, Butterworth filter was used for the noise suppression in a fixed order of 10 and cut off frequencies of 0.38, 0.43, 0.48, 0.53 and 0.58 were used in reconstructing the projection data. Coming after the CT reconstruction, the two images of the different modalities were fused (registered). Furthermore, the OSEM algorithm incorporated corrections for; collimator-specific resolution recovery corrections, scattering corrections, and CT -attenuation corrections.

Computer Aided Detection (CADe) in liver SPECT/CT: CADe is defined as a procedure in medicine that assists doctors in the interpretation of medical images in a higher degree of accuracy within a shortest possible time. Imaging techniques in X-ray, MRI and Ultrasound diagnostics yield a great deal of information which the radiologist has to analyse and evaluate comprehensively in a short time. CADx systems help scan digital images, e.g., from computed tomography, for typical appearances and to highlight conspicuous sections such as potential diseases. Computer aided detection in liver SPECT/CT imaging is aimed at complementing the effort of interpreting physician toward achieving optimal tumour detection. The difference between Computer Aided Diagnosis (CADx) and Computer Aided Detection (CADe) is that CADx deals with tumour characterization while CADe deals with tumour detection[29-31]. The modelled CAD system used in this work comprises of four fundamental components.

Selection of liver area: The reconstruction acquired projection data gave rise to the SPECT images. Image processing software built into the processing computers called xeleris performed the following functions.

Image fusion: The reconstructed liver SPECT image was registered to the sequentially acquired CT image. This gave rise to hardware fusion SPECT/CT image. Furthermore, attenuation, scattering and collimator detector response correction were also made. In summation, an important feature of tumour contouring was also accomplished.

Exclusion of other structures: The xyleris software's function was exploited in excluding all the other structures of the inserts in the phantom other than liver as well as its background.

Segmentation: Segmentation (partitioning) is the procedure of dividing an image into sections with like attributes such as grey level, colour, grain, luminosity, and contrast. The goal of the process is to simplify and/or change the representation of an image into something that is more meaningful and easier. Segmentation process can be achieved by thresholding, edge based detection or region based segmentation. However, thresholding suffers activity inhomogeneity and artefact problems. Consequently in this research we used edge based detection algorithm available on Image J software called find edge menu. The find edges used a Sobel edge detector to highlight sharp changes in intensity in the selection. Two 3×3 convolution kernels (shown below) were applied to generate vertical and horizontal derivatives. The final image was produced by combining the two derivatives using the square root of the sum of the squares:

121	10-1
000	20-2
-1-2-1	10-1

Ultimately, tumour and background area were clearly differentiated.

Volume of interest selection: Following the segmentation process, a clear extent of the tumour was delineated. Thus, a fit eclipses selection menu was used

for the proper marking of the volume of interest. Ultimately, the values depicting the quality of the image were measured and evaluated.

Image J software in statistical analysis and statistical test for SPECT/CT inCAD and non-CAD system: The analysis of the SPECT/CT was also conducted using the open source image processing software (Image J). It is a software base on Java, which was developed at the National Institute of Health, Bethesda, Maryland, USA. Because of its open nature, accessibility to it became easy. However, image processing personal computers give the reconstructed SPECT/CT images' information in DICOM format. This prevented it from losing any of its property. Furthermore, in the process of the analysis, the following basic steps were followed during the analysis:

- The first step was opening the Image J software. This led to the appearance of the tool box with the following labels: File, Edit, Image, Processing, analyse, Plugins, Window and Help
- Click on File→Open→image was selected from the Computer file
- Click on Edit→this was to confirm that the image was in DICOM format
- Click on process Find Edges was selected, it uses a Sobel edge detector to highlight sharp changes in intensity in the active image or extract. This helped accurately tracing tumour edges (a segmentation process)
- Click on Image→Type→select 8-bit→the tumour volume was marked
- Click on image→properties→Set scale→set measurements
- Click analyse→set measurement→measure
- Then the result page will appear. From the result page the were also obtained
- The third batch of the analysis was conducted in the similar manne following measurements were obtained: Mean value, maximum and minimum grey value and standard deviation of the selection among the others
- The same procedure was repeated for another volume of the same magnitude with the background which was selected in the background region immediately close to the tumour, the same statistical measurements r as above. However, the evaluation was done at the exclusion of the segmentation

The t-test (also sometimes called the student t-test) was then used to determine the significance of the difference between the means of the background and tumour for both the segmented and non-segmented images. This test was aimed at comparing their differences in means relative to the observed random variations in tumour and the background. The significance level of 0.05 levels was set, therefore for all the tests, probability (p) values <0.05 were considered statistically significant and the null hypothesis was rejected. The statistical test was conducted Microsoft excel 2007 version, using Independent data and one-sided test selection (one tail distribution). All the data were ensuring to be statistically significant before the image quality evaluation was commenced.

Evaluation of Image quality in SPECT/CT and its parameters: Following the statistical calculations and the statistical tests, SPECT/CT Image quality was evaluated. Because of the tomographic reconstruction process in SPECT/CT image, its noise is no longer Poissonian. In addition, it does not have a uniform (white) power spectrum. Furthermore, it depends on a number of parameters: counts acquired the distribution of the counts, the reconstruction process among the others. Consequently, the raw signal-to-noise ratio is not well behaved and therefore, we used a measure of tomographic contrast, or tomographic contrast-to-noise ratio, in assessing the detectability of the SPECT/CT image. It was calculated using the following formulas. However, the two components of the formula, Contrast and coefficient of variation (which describes the noise) were evaluated first.

Contrast: This refers to the differences in density (or intensity) in parts of the image. It was evaluated using the following relation[13]:

$$\text{Contrast}\,(C) = \frac{\bar{S}-\bar{b}}{\bar{b}}$$

Where:

$\bar{S}$ = The mean value of the high concentration VOI (tumour)

$\bar{b}$ = The mean value of the background VOI

Noise (represented by the background standard deviation): This can be described as an undesirable by-product of image capture that adds spurious and extraneous information. Statistical noise can impair detectability, especially if the object has low contrast. The coefficient of variation (N), also known as "relative variability" which was applied in calculating the CNR, equals the standard deviation divided by the mean. It was expressed as a fraction[13].

$$N = \frac{\sigma b}{\bar{b}}$$

Following the component's evaluation, the essential parameter for evaluating detectability, the CNR (Contrast to Noise Ratio) of the object in the image was then evaluated. The conclusion was reached that, for detectability to be achieved, an object's CNR must exceed 3-5[13]. This condition is known as the Rose criterion[13].

$$\text{Contrast to Noise Ratio}(\text{CNR}) = \frac{C}{N}$$

Where:

N = The noise contrast (coefficient of variation)

σb = The Standard deviation of the liver insert background

$\bar{b}$ = The mean intensity of the background counts

$\bar{S}$ = The mean value of the high concentration VOI (tumour) and C is its contrast

RESULTS AND DISCUSSION

SPECT/CT images showed different but interesting result. The SPECT/CT image quality varies as a consequence of different parameter selection as well as the computing system used in aiding the tumour detection. Established on the types of the reconstruction techniques, FBP reconstructed SPECT/CT showed a less magnitude in terms of the signal and relatively high level of the statistical noise. Its CNR values for all its selected parameters falls below the detection limit set by rose criterion. These include both the computer aided and non-computer aided SPECT/CT images (Fig. 1-3). However, FBP reconstructed SPECT/CT that incorporates Computer aiding system showed an improvement in the magnitude of the CNR compared to the non-aided one (Table 1-4). Furthermore, both the aided and non-aided showed a similar pattern. The CNR value rises initially until it reached a peak at the cutoff frequency 0.48 (Fig. 1-3). The CNR value, then decreases with increasing cutoff frequency.

The quality of SPECT/CT image reconstructed by OSEM algorithm showed an interesting solution. The results showed both the aided and non-aided to have a similar pattern (peak at about three to four numbers of iterations) (Fig. 2 and 4). Nonetheless, the attracting difference is in the range of lesion detection described by the rose criterion (CNR = 3-5). The aided OSEM reconstructed SPECT/CT have its CNR values within the range of detection from 2-8 numbers of iterations (Fig. 2).

Table 1: CNR for CAD FBP reconstructed SPECT/CT (step and shoot acquisition) using 10 subsets versus cut off frequencies

Cut- off frequency	CNR
0.38	1.39
0.43	1.42
0.48	1.69
0.53	1.37
0.58	1.36

Table 2: CNR for CAD OSEM reconstructed SPECT/CT (step and shoot acquisition), 10 subsets versus Numbers of iterations

Iterations	CNR
2	3.71
3	3.84
4	3.89
5	3.67
6	3.58
7	3.38
8	3.17
9	2.57
10	2.01

Table 3: CNR for CAD FBP reconstructed SPECT/CT (step and shoot acquisition) using 10 subsets versus cutoff frequencies

Cut-off frequency	CNR
0.38	1.27
0.43	1.54
0.48	1.68
0.53	1.57
0.58	1.57

Table 4: CNR for OSEM reconstructed SPECT/CT (step and shoot acquisition), 10 subsets versus Numbers of iterations

Iterations	CNR
2	1.68
3	2.27
4	2.04
5	1.57
6	1.51
7	1.47
8	1.47
9	1.39
10	1.38

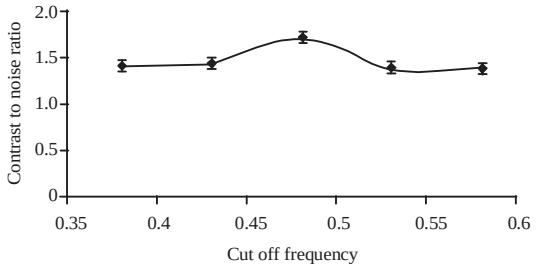

Fig. 1: CNR for CAD FBP reconstructed SPECT/CT (step and shoot acquisition) using 10 subsets versus cutoff frequencies

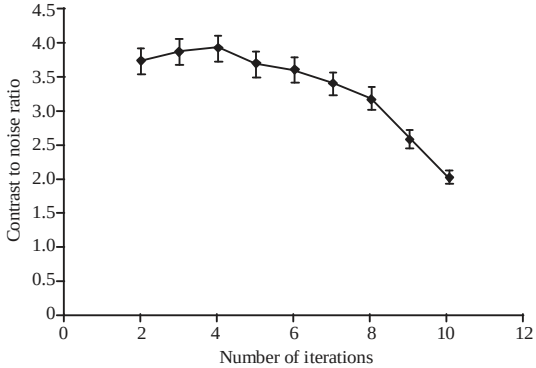

Fig. 2: CNR for CAD OSEM reconstructed SPECT/CT (step and shoot acquisition), 10 subsets versus Numbers of iterations

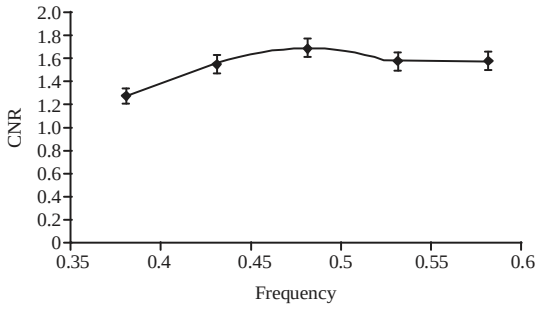

Fig. 3: CNR for FBP reconstructed SPECT/CT (step and shoot acquisition) using 10 subsets versus cut-off frequencies

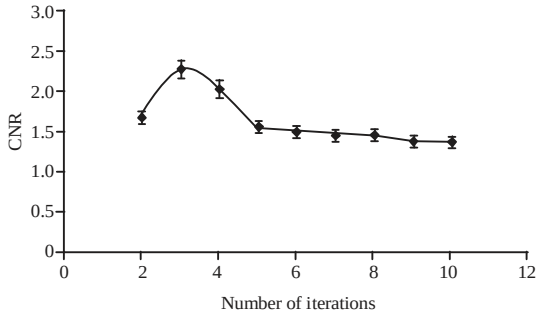

Fig. 4: CNR for CAD OSEM reconstructed SPECT/CT (step and shoot acquisition), 10 subsets versus Numbers of iterations

But, alas for the non-aided one, the CNR values in all the numbers of iteration are below the range of detectability (Fig. 4). This makes the importance of using Computer aided detection apparent. Consequently, tumor detection is achieved with greater accuracy due to the proper segmentation of the liver SPECT/CT image as shown (Fig. 2). The tumour boundary is easily recognized following the utilization of the different intensity, representation in the liver tumour and background (Fig. 5). The variation in the intensity eased the proper marking of the actual extent of the tumour from the overall image. In addition, the achievement was attained at a limited time. Consequently, the examination period reduction added value to CAD incorporated SPECT/CT image. All these were nowhere to be found in case of non-computer aided liver SPECT/CT image.

Ultimately, the result of the liver SPECT/CT image showed the OSEM reconstruction method to be superior to FBP in terms of liver tumour detection (Fig. 2 and 4). In addition, the result easily deduced that the effect of Computer aided detection on Ordered Subset Expectation Maximization (OSEM) is greater compared to Filtered Back Projection (FBP) reconstructed images. Furthermore, the issue of boundary is achieved from the incorporated CT in the image.

SPECT or Planer acquisitions cannot determine the situation of a tumour for better characterization with accuracy[32-34]. The diligence of novel engineering science that combines functional and anatomic information, the SPECT/CT images has proven to improve the detection of liver tumours and other liver abnormalities[35, 36]. Sometimes, accumulation of ^{99m}Tc on the liver surface could be accepted for either planer or SPECT imaging, especially in the case of single tumours. However, only SPECT/CT can detect with greater precision the distribution of the radionuclide in many complicated cases like multiple tumours, metastases, low contrast functional imaging among the others[36]. This results from the low spatial resolution, significant partial volume effect and statistical nature of the radioactive decay that are linked with nuclear medicine imaging in general.

The computer aid detection system has been shown to assist radiologists and other medical imaging interpreters toward achieving greater accuracy compared to the radiologists alone[9]. In the case of liver abnormalities, many studies showed how computer aided detection system improve the quality of medical imaging. However, most of the studies on the liver CAD focus on Computed Tomography (CT) and Magnetic Resonance Imaging (MRI). Several CAD systems for detection and diagnosis were developed by different researchers. Furthermore, these systems all showed an improvement in terms of confidence increment as well as minimization of the reading time.

In the present study, nuclear medicine imaging (SPECT) was used for the evaluation of the modeled CAD system in detecting liver tumour. This is imputable to its capability of detecting abnormality before any anatomical manifestations[14, 37, 38]. The CT image acquisition that was carried out sequentially with the SPECT using the same bed setting gave many advantages. These include; attenuation correction, contouring of the tumour boundary among the others. The study showed a similar result regarding improvement in the interpretation of tumours on liver medical imaging obtained from CT and MRI. The graph pattern showed by FBP reconstructed liver SPECT/CT implies how contrast and noise trade-off is being reached (Fig. 1 and 3). Initially, the noisy liver SPECT was smoothed after applying the Butterworth filter of 0.38 cutoff frequencies to it. This initial application of the filter seriously affected the contrast of the picture. As a result the Contrast to Noise Ratio (CNR) is less. Only as we increased cut-off frequency, the contrast and the spatial resolution improve a little number at the expense of increased interference. However, despite the noise increment and the contrast reduction, the pattern of the graph before the peak implied the dominance of contrast over the noise up to the peak (Fig. 1 and 3). But

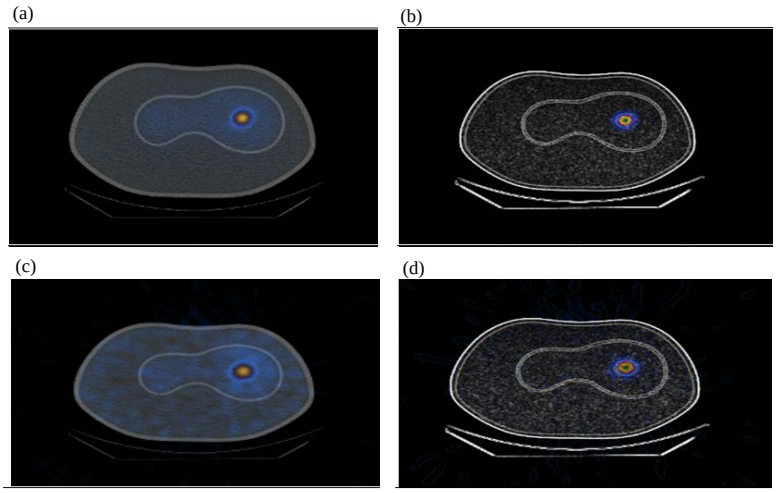

Fig. 5(a-d): (a) Non-segmented OSEM reconstructed liver tumour SPECT, (b) Segmented OSEM reconstructed liver tumour SPECT, (c) Non-segmented FBP liver tumour SPECT and (d) Segmented FBP liver tumour SPECT

at greater cut-off frequencies of 0.53 and above, the noise contribution became greater than the one observed before the peak. Consequently, CNR value decreases after 0.48 cut-off frequencies and above.

In the case of OSEM reconstructed SPECT images (Fig. 2 and 4), the higher frequency noise signals were constantly suppressed by the fixed application of Butterworth filter of 0.48 cutoff frequencies. Nevertheless, the similarity of its graph pattern with that of FBP reconstructed images is explained from a dissimilar view. Granting to the surveys conducted by many researchers, increasing the iteration numbers takes the images closer to the real image. Consequently, spatial resolution and the image contrast increases. Thus, CNR increases with increasing numbers of iterations up to the peak at about 4 numbers of iterations. After the peak it decreases progressively. This is resulted from the fact that, at small numbers of iterations, the increase in high frequency noise is less[13]. Furthermore, the low pass filter (Butterworth) suppressed all the characteristic noisy signals at higher frequencies than its cutoff frequency. Hence, we can also conclude that the trade-off between contrast and noise ratio is also the main determiner. As the numbers of iterations were increased, noise and contrast increases as well. However, before reaching the peak at about 4 numbers of iterations, the contrast is greater than the noise build-up[39-41]. Furthermore, after passing the peak, the noise builds up seems to be dominated relative to the contrast. Consequently, CNR value decreases progressively.

The detection ability based on the limit set by Rose criterion showed that non-computer aided SPECT/CT is not capable of proper detection (Fig. 1 and 2). This is resulted from its failure to reach the CNR value of at least 3.

Therefore, we suggest that CAD system incorporated with SPECT/CT be used in order to achieve a reasonable detection limit. Furthermore, OSEM is the reconstruction algorithm to be constantly used for proper tumor detection. In addition, quantitative evaluation should be used for validating the qualitative evaluation method. This is because qualitative method is characterized by subjectivity. Ultimately, proper interpretation became less reliable, especially in the case of inexperience or less experience radiologist or any other interpreting personnel.

CONCLUSION

CAD in Liver SPECT/CT image achieves its goals by utilizing an OSEM reconstruction algorithm. It is also shown that, qualitative evaluation can be successfully replaced by quantitative one. This would be beneficial to less experience interpreting personnel. Furthermore, in OSEM reconstruction, at around four (4) numbers of iterations, the administered activity of the radionuclide can be brought down. Therefore, the patient and the personnel exposure to radiation would be cut. In addition, above all, incorporating the CAD system in SPECT can prevent any complication in liver SPECT imaging. This is because of its ability to detect the functional and metabolic processes in the liver that normally appears long ago before any anatomical manifestations. In summation, a well-developed CAD system in liver SPECT/CT and other functional and molecular images should be focused by researchers. This would be of great help in the management of almost all the liver related abnormalities at their earliest stage.

ACKNOWLEDGEMENT

The researchers will like to appreciate the role of the entire staff of nuclear medicine unit, AMDI and School of physics, all at the Universiti Sains Malaysia (USM) for their invaluable assistance in this research.

REFERENCES

01. Barbosa, I.R., D.L. de Souza, M.M. Bernal and I. do CC Costa, 2015. Cancer mortality in Brazil: Temporal trends and predictions for the year 2030. Medicine, Vol. 94, 10.1097/MD.0000000000000746
02. O'Keefe, E.L., J.J. DiNicolantonio, H. Patil, J.H. Helzberg and C.J. Lavie, 2016. Lifestyle choices fuel epidemics of diabetes and cardiovascular disease among Asian Indians. Prog. Cardiovasc. Dis., 58: 505-513.
03. Hotez, P.J., M. Alvarado, M.G. Basanez, I. Bolliger and R. Bourne *et al*., 2014. The global burden of disease study 2010: Interpretation and implications for the neglected tropical diseases. PLoS Negl. Trop. Dis., Vol. 8, No. 7. 10.1371/journal.pntd.0002865.
04. Robinson, P.J., P. Arnold and D. Wilson, 2003. Small indeterminate lesions on CT of the liver: A follow-up study of stability. Br. J. Radiol., 76: 866-874.
05. Sahani, D.V., M.A. Bajwa, Y. Andrabi, S. Bajpai and J.C. Cusack, 2014. Current status of imaging and emerging techniques to evaluate liver metastases from colorectal carcinoma. Annl. Surg., 259: 861-872.
06. Young, P.E., C.M. Womeldorph, E.K. Johnson, J.A. Maykel and B. Brucher *et al*., 2014. Early detection of colorectal cancer recurrence in patients undergoing surgery with curative intent: Current status and challenges. J. Can., 5: 262-271.
07. He, G., D. Dhar, H. Nakagawa, J. Font-Burgada and H. Ogata *et al*., 2013. Identification of liver cancer progenitors whose malignant progression depends on autocrine IL-6 signaling. Cell, 155: 384-396.
08. Park, G., Y.K. Kim, C.S. Kim, H.C. Yu and S.B. Hwang, 2010. Diagnostic efficacy of gadoxetic acid-enhanced MRI in the detection of hepatocellular carcinomas: Comparison with gadopentetate dimeglumine. Br. J. Radiol., 83: 1010-1016.
09. Kumar, S.S. and D. Devapal, 2014. Survey on recent CAD system for liver disease diagnosis. Proceedings of the 2014 International Conference on Control, Instrumentation, Communication and Computational Technologies (ICCICCT), July 10-11, 2014, IEEE, Kanyakumari, India, pp: 763-766.
10. Dixit, V. and J. Pruthi, 2014. Review of image processing techniques for automatic detection of tumor in human liver. Int. J. Comput. Sci. Mob. Comput., 3: 371-378.
11. Wang, J.X. and T.T. Zhang, 2009. CT image segmentation by using a FHNN algorithm based on genetic approach. Proceedings of the 2009 3rd International Conference on Bioinformatics and Biomedical Engineering, June 11-13, 2009, IEEE, Beijing, China, pp: 1-4.
12. Sherman, M., J. Bruix, M. Porayko and T. Tran, 2012. Screening for hepatocellular carcinoma: The rationale for the American Association for the study of liver diseases recommendations. Hepatol., 56: 793-796.
13. Cherry, S.R., J.A. Sorenson and M.E. Phelps, 2012. Physics in Nuclear Medicine. 4th Edn., Elsevier, Philadelphia, Pennsylvania, Pages: 523.
14. Powsner, R.A. and E.R. Powsner, 2008. Essential Nuclear Medicine Physics. John Wiley & Sons, New York, USA.,.
15. Gates, V.L., N. Singh, R.J. Lewandowski, S. Spies and R. Salem, 2015. Intraarterial hepatic SPECT/CT imaging using ^{99m}Tc-macroaggregated albumin in preparation for radioembolization. J. Nucl. Med., 56: 1157-1162.
16. Groheux, D., S. Giacchetti, M. Delord, E. Hindie and L. Vercellino *et al*., 2013. 18F-FDG PET/CT in staging patients with locally advanced or inflammatory breast cancer: Comparison to conventional staging. J. Nucl. Med., 54: 5-11.
17. Shah, K., V. Gendel, M. Becker and J. Kempf, 2015. 99m Technetium-Macroaggregated Albumin (MAA) SPECT/CT liver perfusion imaging prior to radioembolization: Patterns and pitfalls of extrahepatic activity. J. Nucl. Med., 56: 1876-1876.
18. Ritt, P., J. Sanders and T. Kuwert, 2014. SPECT/CT technology. Clin. Trans. Imaging, 2: 445-457.
19. Schillaci, O., 2005. Hybrid SPECT/CT: A new era for SPECT imaging?. Eur. J. Nucl. Med. Mol. Imaging, 32: 521-524.
20. Sharma, P., V.S. Dhull, S. Jeph, R.M. Reddy and H. Singh *et al*., 2013. Can hybrid SPECT-CT overcome the limitations associated with poor imaging properties of 131I-MIBG?: Comparison with planar scintigraphy and SPECT in pheochromocytoma. Clin. Nucl. Med., 38: e346-e353.
21. Patton, J.A. and T.G. Turkington, 2008. SPECT/CT physical principles and attenuation correction. J. Nucl. Med. Technol., 36: 1-10.
22. Ruf, J., D. Seehofer, T. Denecke, L. Stelter, N. Rayes, R. Felix and H. Amthauer, 2007. Impact of image fusion and attenuation correction by SPECT-CT on the scintigraphic detection of parathyroid adenomas. Nuklearmedizin, 46: 15-21.
23. Ahmadzadehfar, H., H. Duan, A.R. Haug, S. Walrand and M. Hoffmann, 2014. The role of SPECT/CT in radioembolization of liver tumours. Eur. J. Nuclear Med. Mol. Imaging, 41: 115-124.

24. Ahmadzadehfar, H. And H.J. Biersack, 2013. Clinical Applications of SPECT-CT. Springer Science & Business Media, Berlin, Germany,.
25. Ahmadzadehfar, H. and M. Hoffmann, 2014. Therapy Planning with SPECT/CT in Radioembolisation of Liver Tumours. In: Clinical Applications of SPECT-CT, Ahmadzadehfar, H. and H.J. Biersack (Eds.)., Springer, Berlin, Germany, pp: 255-270.
26. Leal, J., S. Rowe and R. Wahl, 2014. Performance comparison of Auto-PERCIST (a semi-automated PERCIST-based CAD system) and a clinician in the measurement of PERCIST 1.0 metrics for response assessment. J. Nucl. Med., 55: 2073-2073.
27. Charman, W.N., 1998. Imaging in the 21st century. Ophthalmic Physiol. Opt., 18: 210-223.
28. Mettler Jr., F.A. and M.J. Guiberteau, 2011. Essentials of Nuclear Medicine Imaging. Elsevier, New York, USA.,.
29. Suzuki, K., 2012. A review of computer-aided diagnosis in thoracic and colonic imaging. Quant. Imaging Med. Surg., 2: 163-176.
30. Doi, K., 2005. Current status and future potential of computer-aided diagnosis in medical imaging. Br. J. Radiol., 78: s3-s19.
31. Bogoni, L., P. Cathier, M. Dundar, A. Jerebko and S. Lakare *et al*., 2005. Computer-aided detection (CAD) for CT colonography: A tool to address a growing need. Br. J. Radiol., 78: S57-S62.
32. Aparici, C.M., A.M. Avram, A.S. Castrejon, R.A. Dvorak and P. Erba *et al*., 2011. SPECT-CT for Tumor Imaging. In: Atlas of SPECT-CT, Fanti, S., M. Farsad and L. Mansi (Eds.)., Springer, Berlin, Germany, pp: 15-104.
33. Keidar, Z., O. Israel and Y. Krausz, 2003. SPECT/CT in tumor imaging: Technical aspects and clinical applications. Semin. Nucl. Med., 33: 205-218.
34. Lavely, W.C., S. Goetze, K.P. Friedman, J.P. Leal and Z. Zhang *et al*., 2007. Comparison of SPECT/CT, SPECT and planar imaging with single-and dual-phase 99mTc-sestamibi parathyroid scintigraphy. J. Nucl. Med., 48: 1084-1089.
35. Kim, E.E., 2014. Clinical applications of SPECT-CT. J. Nucl. Med., 55: 2078-2078.
36. Mariani, G., L. Bruselli, T. Kuwert, E.E. Kim and A. Flotats *et al*., 2010. A review on the clinical uses of SPECT/CT. Eur. J. Nucl. Med. Mol. Imaging, 37: 1959-1985.
37. Fanti, S., M. Farsad and L. Mansi, 2011. Atlas of SPECT-CT. Springer, Berlin, Germany,.
38. Groch, M.W. and W.D. Erwin, 2000. SPECT in the year 2000: Basic principles. J. Nucl. Med. Technol., 28: 233-244.
39. Koch, W., C. Hamann, J. Welsch, G. Popperl, P.E. Radau and K. Tatsch, 2005. Is iterative reconstruction an alternative to filtered backprojection in routine processing of dopamine transporter SPECT studies?. J. Nucl. Med., 46: 1804-1811.
40. McConnell, D., B. Kemp, C. Hunt, G. Johnson and V. Lowe, 2012. Evaluation of an iterative reconstruction algorithm that models the detector response of the PET scanner. J. Nucl. Med., 53: 2618-2618.
41. Nichols, K.J., G.G. Tronco and C.J. Palestro, 2015. Effect of reconstruction algorithms on the accuracy of 99mTc sestamibi SPECT/CT parathyroid imaging. Am. J. Nucl. Med. Mol. Imaging, 5: 195-203.